

# Small-signal model parameter extraction for microwave SiGe HBTs based on $Y$ - and $Z$ -parameter characterization

Fu Jun(付军)<sup>†</sup>

(Tsinghua National Laboratory for Information Science and Technology (TNList), Institute of Microelectronics, Tsinghua University, Beijing 100084, China)

**Abstract:** High frequency intrinsic small-signal model parameter extraction for microwave SiGe heterojunction bipolar transistors is studied, with a focus on the main feedback elements including the emitter series resistor, internal and external base–collector capacitors as well as the base series resistor, all of which are important in determining the behavior of the device equivalent circuit. In accordance with the respective features of definition of the  $Y$ - and  $Z$ -parameters, a novel combined use of them succeeds in reasonably simplifying the device equivalent circuit and thus decoupling the extraction of base–collector capacitances from other model parameters. As a result, a very simple direct extraction method is proposed. The proposed method is applied for determining the SiGe HBT small-signal model parameters by taking numerically simulated  $Y$ - and  $Z$ -parameters as nominal “measurement data” with the help of a Taurus-device simulator. The validity of the method is preliminarily confirmed by the observation of certain linear relations of device frequency behavior as predicted by the corresponding theoretical analysis. Furthermore, the extraction results can be used to reasonably account for the dependence of the extracted model parameters on device geometry and process parameters, reflecting the explicit physical meanings of parameters, and especially revealing the distributed nature of the base series resistor and its complex interactions with base–collector capacitors. Finally, the accuracy of our model parameter extraction method is further validated by comparing the modeled and simulated  $S$ -parameters as a function of frequency.

**Key words:** SiGe; heterojunction bipolar transistors; small-signal; model; parameter extraction

**DOI:** 10.1088/1674-4926/30/8/084005

**EEACC:** 1350F; 2560B; 2560J

## 1. Introduction

For silicon bipolar junction transistors (BJTs) and silicon–germanium (SiGe) or III–V group heterojunction bipolar transistors (HBTs) in high speed and microwave frequency applications, small-signal equivalent circuit modeling and parameter extraction are known to be the cornerstone for corresponding circuit simulation and design. Moreover, the extracted values for some of the model parameters, e.g. base series resistances and base–collector capacitances, can be conveniently taken as process characteristic metrics for evaluating the high speed or high frequency performance of the relevant technologies.

Over the past few years, a variety of methods for BJT/HBT high frequency small-signal modeling and parameter extraction have been studied and developed<sup>[1–12]</sup>. On the whole, two aspects of work are involved, or more exactly, mixed up in the above mentioned parameter extraction, i.e. determination of values for intrinsic and extrinsic elements, respectively, in the small-signal equivalent circuit of a device.

As for intrinsic part modeling, the determination of base resistances and collector-base capacitances remained a challenge because of their distributed nature and complex interaction. The so-called input impedance method<sup>[13]</sup>, the most

traditional approach to extracting the base resistance of the small-signal equivalent circuit for a BJT, may not be competent enough for accurate modeling as a result of ignoring the effect of base–collector capacitances. Early in 1991, Nakadai *et al.*<sup>[1]</sup> published a method of measuring the base resistance of bipolar transistors based on  $Y$ -parameter analysis considering influences of both internal and external base–collector capacitors. Nevertheless, the emitter series resistor as an important feedback element in common-emitter circuit configuration was not considered in this method, limiting its application in practice. For ease of processing for all series resistors, a new BJT small-signal parameter extraction technique was later presented on the basis of  $Z$ -parameter characterization<sup>[3]</sup>. Though the internal base–collector capacitor can be directly extracted, this approach has to rely on numerical optimization if the external base–collector capacitor needs to be included in the small-signal equivalent circuit. In Ref. [5], Ouslimani *et al.* demonstrated direct extraction of all the HBT small-signal parameters covering external as well as internal base–collector capacitors using analytical expressions, at the expense, however, of high computation complexity.

Regarding extrinsic parameter extraction, on the one hand, various pad deembedding techniques have been widely used. Nevertheless, there always exist not only deembedding

<sup>†</sup> Corresponding author. Email: fujun@mail.tsinghua.edu.cn

Received 8 January 2009, revised manuscript received 16 March 2009

© 2009 Chinese Institute of Electronics

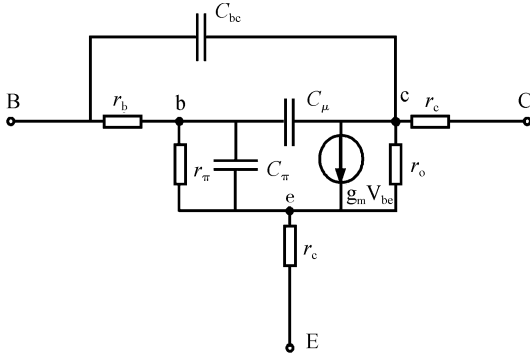


Fig. 1. Common-emitter hybrid  $\pi$ -mode high frequency small-signal equivalent circuit of the intrinsic part of an SiGe HBT.

errors, but also certain extrinsic parasitics e.g. collector-to-substrate capacitances cannot be deembedded at all through the use of industry standard dummy test structures. On the other hand, although most of the extrinsic parasitic elements can normally be determined by biasing the device in “hot” (overdriven) or/and “cold” (cut-off) operation<sup>[4,6,8–12]</sup>, this kind of technique is unsuitable for extracting bias dependent extrinsic parameters. Therefore, in Ref. [7], this kind of technique was applied in conjunction with the use of dummy structures for deembedding correction. No doubt, anyway, the imperfect deembedding and extrinsic parameter determination will in turn interfere with the intrinsic small-signal modeling parameter extraction, and even may cover up the physical nature of device modeling to a great degree. In this sense, the separation of intrinsic parameter extraction from extrinsic parasitics determination is necessary.

The purpose of this work is to explore physical insights into the device modeling of intrinsic small-signal equivalent circuits for SiGe HBTs, while leaving parasitic extrinsic elements and associated deembedding techniques beyond the scope of this paper. As we know, a device simulator is a good choice for creating an ideal device architecture excluding any extrinsic elements which may otherwise be difficult or even impossible to filter from an actual measurement set-up. So, in order to eliminate interference from extrinsic elements with the intrinsic part of a device equivalent circuit, numerical simulation results instead of real measurement data are used for parameter extraction in this paper. Based on the simulation data, through the combination of  $Y$ - and  $Z$ -parameter characterization and reasonable approximation, a simple direct extraction method is proposed to extract small-signal model parameters including base and emitter series resistances, and external and internal base–collector capacitances, for SiGe HBTs.

## 2. Theory

After leaving out all of the extrinsic parasitic elements, as illustrated in Fig. 1, the common-emitter (CE) hybrid  $\pi$ -mode high frequency small-signal equivalent circuit of the intrinsic part of a SiGe HBT is investigated, with a focus on base series

resistor  $r_b$  and important feedback elements including emitter series resistor  $r_e$ , internal component  $C_\mu$  and external component  $C_{bc}$  of the base–collector capacitor. The other elements  $r_\pi$ ,  $C_\pi$ ,  $r_o$  and  $r_c$  in the schematic have their normal meanings. In addition, transconductance  $g_m$  characterizing the voltage-controlled current source can be related to DC transconductance  $g_{m0}$  ( $= qI_C/K_B T$ ) as below<sup>[14]</sup>:

$$g_m = g_{m0} \exp(-j\omega\tau_d) \approx \frac{qI_C}{k_B T} (1 - j\omega\tau_d), \quad (1)$$

where  $\omega$  is the angular frequency, and  $\tau_d$  stands for the transit time phase delay of the transconductance.

The examination of the circuit in Fig.1 indicates that the presence of the feedback capacitors  $C_\mu$  and  $C_{bc}$  spanning across input and output makes it difficult to formulate the small-signal model analytically. On the other hand, even if normally the values for  $C_\mu$  and  $C_{bc}$  may be much less than  $C_\pi$ , neither of them can be neglected arbitrarily due to the well-known Miller effect. In other words, seen from the input point of view, the feedback capacitances will be approximately magnified by a large factor of  $1 + |A_v|$  if e.g. the output is left open-circuited, resulting in a high value of the small-signal voltage magnification  $A_v$ . It is worth noting that, nevertheless, if the output (collector terminal) is shorted to ground (emitter terminal), the Miller effect will be greatly alleviated because of the nearly zero value of  $A_v$  in this case. Consequently, when characterizing the device using  $Y$ -parameters which are defined under a short-circuited port condition, the small-signal equivalent circuit can be reasonably simplified by removing the base–collector capacitors. Furthermore, as the output resistor  $r_o$  is normally large enough (in view of the very large values of Early voltages for SiGe HBTs) to be neglected from the above simplified circuit, one can obtain the following relations based on  $Y$ -parameter characterization.

$$\text{Re} \left( \frac{y_{11}}{y_{21}} \right) = \frac{1}{g_{m0} r_\pi} - \frac{\tau_d C_\pi}{g_{m0}} \omega^2, \quad (2)$$

$$\text{Im} \left( \frac{y_{11}}{y_{21}} \right) = \frac{C_\pi + \frac{\tau_d}{r_\pi}}{g_{m0}} \omega, \quad (3)$$

$$\text{Re} \left( \frac{1}{y_{21}} \right) = r_e + \frac{1 + \frac{r_b + r_e}{r_\pi}}{g_{m0}} - \frac{(r_b + r_e) C_\pi \tau_d}{g_{m0}} \omega^2. \quad (4)$$

According to the above formulae, the linear regression of  $\text{Re}(y_{11}/y_{21})$  and  $\text{Re}(1/y_{21})$  with respect to  $\omega^2$  and the linear regression of  $\text{Im}(y_{11}/y_{21})$  versus  $\omega$ , respectively, will determine both slopes and intercepts of these linear relations, leading to altogether five equations, which can just be combined to solve for the five unknown small-signal model parameters  $r_b$ ,  $r_e$ ,  $r_\pi$ ,  $C_\pi$  and  $\tau_d$ .

We now turn to the  $Z$ -parameters which are defined with input and output kept open-circuited, respectively. Because of the severe Miller effect in this case, neither  $C_\mu$  nor  $C_{bc}$  can be

ignored any more. Although it is generally hard to derive compact closed-form expressions of  $Z$ -parameters for the equivalent circuit with the addition of  $C_\mu$  and  $C_{bc}$  as shown in Fig. 1, differences of some  $Z$ -parameters such as  $z_{11} - z_{12}$  and  $z_{22} - z_{21}$  can still be expressed analytically as below through application of the theorem of circuitry superposition.

$$\operatorname{Re}\left(\frac{1}{z_{11} - z_{12}}\right) = \frac{1 + \frac{C_{bc}}{C_\mu}}{r_b}, \quad (5)$$

$$\frac{1}{\operatorname{Im}(z_{22} - z_{21})} = -\left(C_\mu + C_{bc}\right)\omega - \frac{r_b^2 C_\mu^2 C_{bc}^2}{C_\mu + C_{bc}}\omega^3. \quad (6)$$

As will be demonstrated in Section 4, the second term is normally negligibly small compared to the first one at frequencies of interest in the right-hand side of the above expression, so it can be approximated as below.

$$\frac{1}{\operatorname{Im}(z_{22} - z_{21})} \approx -\left(C_\mu + C_{bc}\right)\omega. \quad (7)$$

Obviously from Eq. (7), the linear dependence of  $1/\operatorname{Im}(z_{22} - z_{21})$  on  $\omega$  can be used to determine the value of the slope i.e.  $-(C_\mu + C_{bc})$ . In combination with Eq. (5) where  $r_b$  has already been extracted, the internal and external base-collector capacitances can be obtained in the end.

To sum up, owing to the combination of  $Y$ - and  $Z$ -parameter characterization, a very simple direct extraction method is proposed here while taking all the main feedback elements ( $C_\mu$ ,  $C_{bc}$  and  $r_e$ ) as well as base series resistor  $r_b$  into account.

### 3. Simulation

In this work, the simulation of a SiGe HBT with a numerical device simulator Taurus-device<sup>[15]</sup> is used to provide the relevant small-signal  $Y$ - and  $Z$ -parameters required for the model parameter extraction.

The cross-section of the SiGe HBT device architecture for simulation is schematically shown in Fig. 2, where only the right half is taken in view of the device symmetry. The geometry and process details are summarized below. On top of a  $2\ \mu\text{m}$  thick lightly doped  $n$ -type epitaxial layer, a  $p$ -type-doped base Si/SiGe/Si stack epitaxial layer with a total thickness of  $55\ \text{nm}$  is placed. In addition, heavily doped  $n^+$  and  $p^+$  ohmic regions are introduced at the surface of the device as emitter and external base contacts, respectively. Meanwhile, another  $n^+$  division at the backside of the device is used to construct the collector contact. The emitter, base and collector electrodes are tied to the corresponding contacts. All of the doping concentration profiles in the contact regions and inside the Si/SiGe/Si epitaxial layer are created according to the Gauss distribution function. Also, trapezoidal Ge distribution is employed with top plateau Ge percentage being 20%. Correspondingly, the vertical profiles of Ge mole fraction and impurity density along the cutline through the center of the

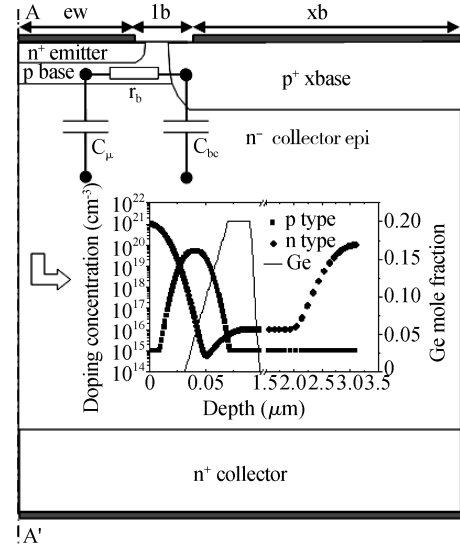


Fig. 2. Device architecture of an SiGe HBT for simulation with only right half taken considering the device symmetry.

emitter are also shown in the inset of the figure. Regarding lateral dimensions, as labeled inside Fig. 2, the widths of the emitter and base electrodes are denoted as  $ew$  and  $xb$ , respectively, with the link-up base width  $lb$  defined as the distance between them. It should be noted that, unless otherwise stated,  $ew = 0.55\ \mu\text{m}$ ,  $lb = 0.3\ \mu\text{m}$ ,  $xb = 1.35\ \mu\text{m}$ ,  $n$ -epi doping concentration  $N_{\text{epi}} = 1 \times 10^{16}\ \text{cm}^{-3}$  and top plateau base doping concentration  $N_B = 5 \times 10^{19}\ \text{cm}^{-3}$  are used for simulation with the total device width (along the direction perpendicular to the cross-section) fixed at  $1\ \mu\text{m}$ .

An AC small-signal simulation on the above defined device structure was carried out under bias conditions of  $V_{be} = 0.85\ \text{V}$  and  $V_{ce} = 5\ \text{V}$  at frequencies ranging from  $0.125$  to  $2\ \text{GHz}$ . During the simulation, physical models of bandgap narrowing induced by Ge content as well as the heavy doping effect, Hansch field dependent carrier mobility and impurity concentration dependent SRH and Auger recombination are employed by the Taurus-device simulator<sup>[15]</sup>. Finally, the simulated  $Y$ - and  $Z$ -parameters are collected for the subsequent small-signal parameter extraction.

### 4. Results and discussion

Based on these  $Y$ - and  $Z$ -parameters obtained from numerical high frequency small-signal simulation of the SiGe HBT as illustrated in Fig. 2, the left hand side of the expressions of Eqs. (2)–(4), Eq. (5) and Eq. (7) are calculated and used to plot the corresponding curves as a function of  $\omega^2$  or  $\omega$ , respectively, in Figs. 3, 4, and 5. As shown in Fig. 3, it is clear that both  $\operatorname{Re}(y_{11}/y_{21})$  and  $\operatorname{Re}(1/y_{21})$  exhibit descending linear dependence on  $\omega^2$ , just as predicted by Eq. (2) and Eq. (4), respectively. Meanwhile, Figure 4 clearly shows an ascending relation of  $\operatorname{Im}(y_{11}/y_{21})$  in direct proportion to  $\omega$ , in accordance with Eq. (3). On the other hand, as can be seen from Fig. 5,  $\operatorname{Re}(1/(z_{11} - z_{12}))$  manifests itself nearly as a constant independent of  $\omega$  while  $1/\operatorname{Im}(z_{22} - z_{21})$  decreases directly proportional

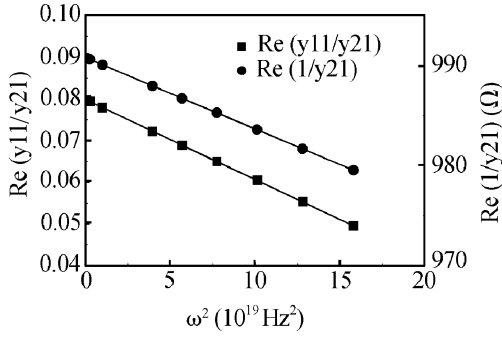


Fig. 3.  $\text{Re}(y_{11}/y_{21})$  and  $\text{Re}(1/y_{21})$  versus  $\omega^2$  calculated from high frequency small-signal simulation results simulated by a Taurus-device simulator for the SiGe HBT as illustrated in Fig. 2.

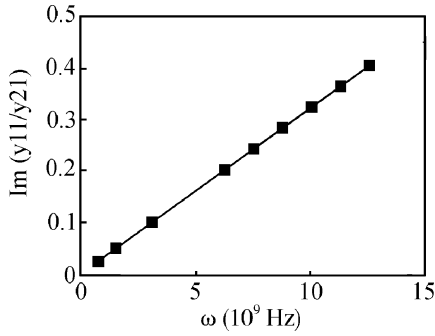


Fig. 4.  $\text{Im}(y_{11}/y_{21})$  versus  $\omega$  calculated from high frequency small-signal simulation results simulated by a Taurus-device simulator for the SiGe HBT as illustrated in Fig. 2.

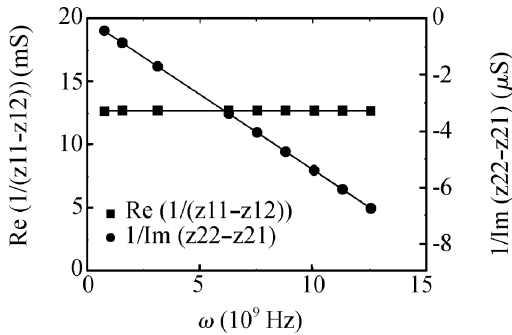


Fig. 5.  $\text{Re}(1/(z_{11} - z_{12}))$  and  $1/\text{Im}(z_{22} - z_{21})$  versus  $\omega$  calculated from high frequency small-signal simulation results simulated by a Taurus-device simulator for the SiGe HBT as illustrated in Fig. 2.

to  $\omega$  with a negative slope, in good agreement with prediction given by Eq. (5) and Eq. (7), respectively. As a consequence, the theoretical analysis given in Section 2, as a basis of the method proposed for extracting the small-signal equivalent circuit model parameters of the SiGe HBT, has been justified, at least to some extent, by the device simulation.

From the plots of Figs. 3, 4, and 5, the linear regression lines are derived and drawn together with the simulation data symbols as shown in these figures, from which the linear regression slopes and intercepts can be readily determined. Therefore, the small-signal equivalent circuit model parameters have been extracted in this simple manner, with a focus upon analysis of  $r_b$ ,  $r_e$ ,  $C_\mu$ , and  $C_{bc}$  below in this section.

The extracted values for the base-collector capacitors are plotted as a function of n- collector epi doping concen-

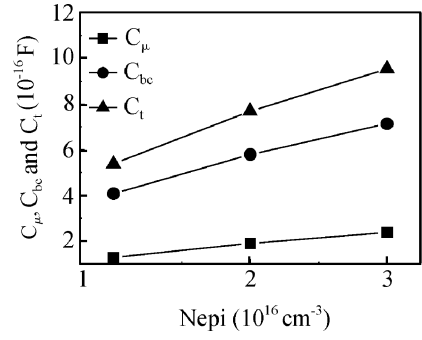


Fig. 6. Variation of extracted base-collector capacitances (internal  $C_\mu$ , external  $C_{bc}$  and total  $C_t$ ) with doping concentration of n- epitaxial layer  $N_{epi}$  for the SiGe HBT as illustrated in Fig. 2.

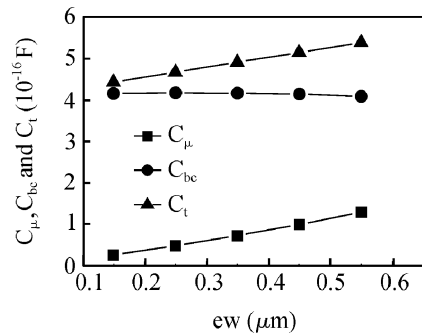


Fig. 7. Variation of extracted base-collector capacitances (internal  $C_\mu$ , external  $C_{bc}$  and total  $C_t$ ) with emitter width  $ew$  for the SiGe HBT as illustrated in Fig. 2.

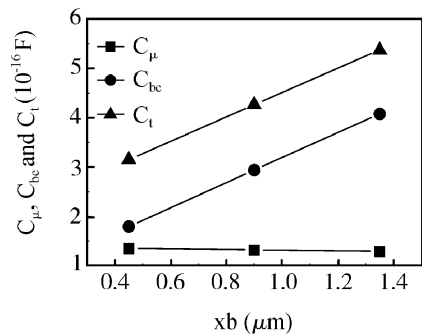


Fig. 8. Variation of extracted base-collector capacitances (internal  $C_\mu$ , external  $C_{bc}$  and total  $C_t$ ) with external base width  $xb$  for the SiGe HBT as illustrated in Fig. 2.

tration  $N_{epi}$ , emitter width  $ew$ , and external base width  $xb$  in Figs. 6, 7 and 8, respectively. Beginning with Fig. 6, the extracted values of  $C_\mu$ ,  $C_{bc}$  and their sum  $C_t = (C_\mu + C_{bc})$  reflect a reasonable increase in base-collector p-n junction capacitances with  $N_{epi}$ . Apparently it would be beneficial in the reduction of base-collector capacitances to adopt as lightly doped a collector epi as possible. Then, as shown in Fig. 7,  $C_\mu$  decreases in direct proportion to the shrinking emitter width and at the same time  $C_{bc}$  is found to remain almost unchanged with  $ew$  shrinkage. In contrast, Figure 8 shows that  $C_\mu$  is hardly affected by variation in  $xb$  while  $C_{bc}$  follows a decreasing linear tendency as  $xb$  narrows. The observed dependence of  $C_\mu$  and  $C_{bc}$  agrees well with the splitting of the base-collector capacitor defined in the equivalent circuit, reflecting an explicit and reasonable physical meaning

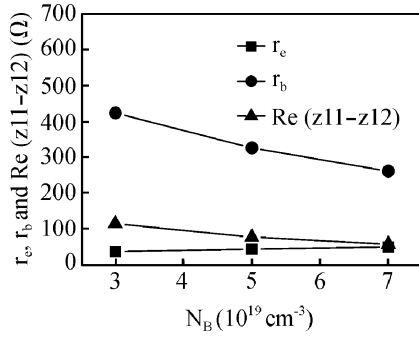


Fig. 9. Variation of extracted base and emitter series resistances  $r_b$  and  $r_e$  with top plateau base doping concentration  $N_B$  for the SiGe HBT as illustrated in Fig. 2.

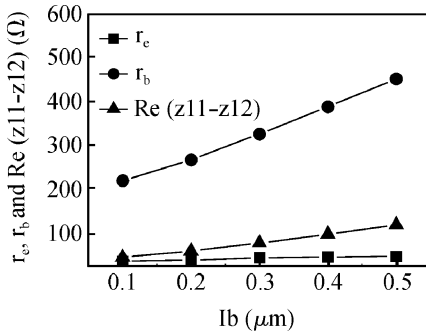


Fig. 10. Variation of extracted base and emitter series resistances  $r_b$  and  $r_e$  with link-up base width  $l_b$  for the SiGe HBT as illustrated in Fig. 2.

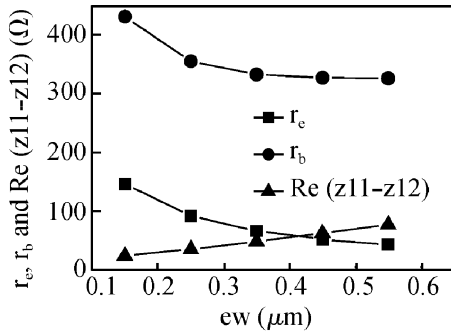


Fig. 11. Variation of extracted base and emitter series resistances  $r_b$  and  $r_e$  with emitter width  $ew$  for the SiGe HBT as illustrated in Fig. 2.

of our method. In fact, as illustrated in Fig. 2,  $C_\mu$  and  $C_{bc}$  can be regarded approximately as capacitance components of the internal (proportional to  $ew$ ) and external (proportional to  $xb$ ) base region with n-collector epi, respectively, with  $r_b$  linking base terminals of the two capacitors. Consequently, the necessity and rationality of splitting the base-collector capacitor as shown in Fig. 2 have been verified here from a device physics point of view.

On the other hand, the extracted base and emitter series resistances  $r_b$  and  $r_e$  are compared for different top plateau base doping concentrations ( $N_B$ ), link-up base widths ( $l_b$ ), and emitter widths ( $ew$ ) in Figs. 9, 10, and 11, respectively. Firstly, as depicted in Fig. 9, it is easy to understand that little change in  $r_e$  and simultaneously noticeable reduction in  $r_b$  with increasing  $N_B$  are observed. This is why nowadays much heavier base doping level than ever has been used in advanced

SiGe HBT technologies for reducing base resistance and thus improving high frequency gain and noise performance. Secondly, in Fig. 10  $r_e$  is kept nearly as an invariable, of course, regardless of  $l_b$  variation, while  $r_b$  can be effectively reduced as  $l_b$  diminishes. This is one of the most important reasons why self-aligned emitter-base architecture needs to be adopted for building high performance BJT or HBT devices. Finally, as can be easily seen, in Fig. 11  $r_e$  is found to go up on reducing  $ew$  as a result of being inversely proportional to the emitter width. Also in Fig. 11, however, as  $ew$  decreases, the extracted  $r_b$  is discovered to increase somewhat in the beginning and even accelerate to rise after  $ew$  gets smaller than  $0.35 \mu\text{m}$  or so, which seems to contradict common sense of base resistance reduction with down-scaling  $ew$ . In contrast, if following  $r_b = \text{Re}(z_{11}-z_{12})$  in Ref. [3], the extracted base resistance values are shown in Fig. 11 to be consistent with plausible common sense. It should be noted, nevertheless, that common sense does not always tell the truth. Keep in mind that the expression  $r_b = \text{Re}(z_{11}-z_{12})$  was derived in Ref. [3] in the absence of  $C_{bc}$ . In fact, based on the analysis in Section 2 taking the influence of  $C_{bc}$  into account, the expression of  $\text{Re}(z_{11}-z_{12})$  can be given by

$$\text{Re}(z_{11} - z_{12}) = \frac{r_b \left(1 + \frac{C_{bc}}{C_\mu}\right)}{\left(1 + \frac{C_{bc}}{C_\mu}\right)^2 + \omega^2 r_b^2 C_{bc}^2}. \quad (8)$$

Hence, due to  $\omega^2 r_b^2 C_{bc}^2 \ll \left(1 + \frac{C_{bc}}{C_\mu}\right)^2$  over the frequency range of interest, the relation between  $r_b$  and  $\text{Re}(z_{11}-z_{12})$  can be rearranged as follows.

$$r_b \approx \left(1 + \frac{C_{bc}}{C_\mu}\right) \text{Re}(z_{11} - z_{12}). \quad (9)$$

Obviously, Equation (9) would be reduced to the expression used by Ref. [3] if  $C_{bc}$  was set to zero. According to Eq. (9), in view of the existence of  $C_{bc}$ ,  $r_b$  is approximately equal to  $\text{Re}(z_{11}-z_{12})$  multiplied by a factor of  $\left(1 + \frac{C_{bc}}{C_\mu}\right)$ . As a result, the decreasing tendency of  $\text{Re}(z_{11}-z_{12})$  with decreasing  $ew$  would actually be offset and even reversed by the  $C_\mu$  reduction caused by  $ew$  shrinkage, leading to the resultant increasing  $r_b$  with narrowing  $ew$  as shown in Fig. 11. Essentially the above observed seemingly abnormal  $r_b$  variation with  $ew$  can be ascribed to the complicated distributed nature of the base resistor in the SiGe HBT. Furthermore, sloppy omission of  $C_{bc}$  or improper splitting of the base-collector capacitor may in turn result in incorrect  $r_b$  determination.

Finally, all of the four high frequency  $S$ -parameters are calculated by using an Agilent ADS circuit simulator with the above extracted model parameters substituted into the small-signal equivalent circuit. The calculated  $S_{11}$ ,  $S_{22}$ ,  $S_{21}$  and  $S_{22}$ , both in the form of magnitude and angle, as a function of frequency, are given in Fig. 12 through Fig. 15, in comparison to the Taurus-device numeric simulation results, on which the

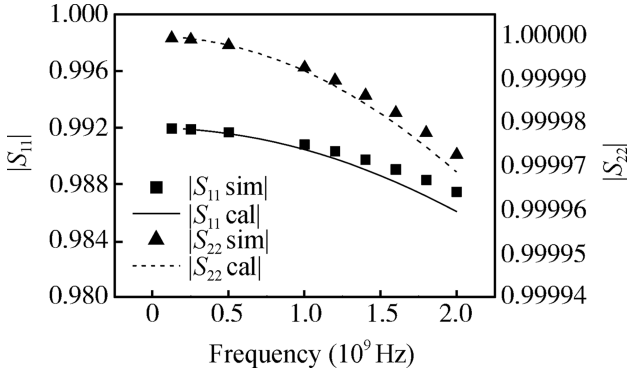


Fig. 12. Magnitudes of  $S_{11}$  and  $S_{22}$  versus frequencies calculated with an ADS circuit simulator based on our model compared with the corresponding simulation results given by a Taurus-device simulator for the SiGe HBT as illustrated in Fig. 2.

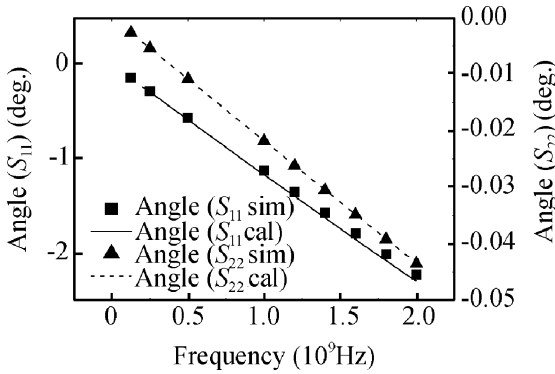


Fig. 13. Angles of  $S_{11}$  and  $S_{22}$  versus frequencies calculated with an ADS circuit simulator based on our model compared with the corresponding simulation results given by a Taurus-device simulator for the SiGe HBT as illustrated in Fig. 2.

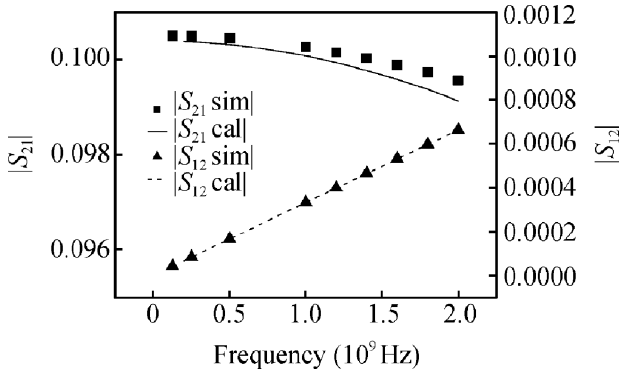


Fig. 14. Magnitudes of  $S_{21}$  and  $S_{12}$  versus frequencies calculated with an ADS circuit simulator based on our model compared with the corresponding simulation results given by a Taurus-device simulator for the SiGe HBT as illustrated in Fig. 2.

device model parameter extraction is based. It is worth mentioning here that the value of collector series resistance  $r_c$ , which is necessary for ADS calculation, is estimated following Eq. (6) in Ref. [3], i.e.

$$r_c = \text{Re}(z_{22} - z_{21}). \quad (10)$$

As shown in Figs. 12–15, the calculated curves are found to be in good agreement with the corresponding simulated

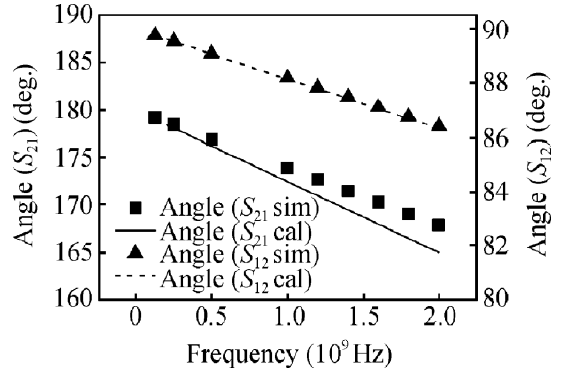


Fig. 15. Angles of  $S_{21}$  and  $S_{12}$  versus frequencies calculated with an ADS circuit simulator based on our model compared with the corresponding simulation results given by a Taurus-device simulator for the SiGe HBT as illustrated in Fig. 2.

results, thus further validating our model parameter extraction method.

### 5. Conclusions

In this paper, a simple method is proposed to directly extract high frequency CE hybrid- $\pi$  mode small-signal model parameters for microwave SiGe HBTs, with a focus on the main feedback elements including the emitter series resistor, internal and external base–collector capacitors as well as the base series resistor in the device equivalent circuit. A novel combined use of  $Y$ - and  $Z$ -parameters enables reasonable simplification of the device equivalent circuit and thus decoupling the extraction of base–collector capacitances from other model parameters. As a result, the parameter extraction is greatly simplified through two-step  $Y$ - and  $Z$ -parameter characterization. The validity of the method is preliminarily confirmed by using numerical device simulation data for extracting the corresponding model parameters. Furthermore, the extraction results can be used to reasonably account for the dependence of the extracted model parameters on device geometry and process parameters, reflecting the explicit physical meanings of parameters, and especially revealing the distributed nature of the base series resistor and its complex interactions with base–collector capacitors. Finally, the accuracy of our model parameter extraction method is further validated by comparing the modeled and simulated  $S$ -parameters as a function of frequency.

### References

- [1] Nakadai T, Hashimoto K. Measuring the base resistance of bipolar transistors. IEEE Bipolar Circuits and Technology Meeting, 1991: 200
- [2] Pehlke D R, Pavlidis D. Direct calculation of the HBT equivalent circuit from measured  $S$ -parameters. IEEE MTT-S Digest, 1992: 735
- [3] Lee S, Ryum B R, Kang S W. A new parameter extraction technique for small-signal equivalent circuit of polysilicon emitter bipolar transistors. IEEE Trans Electron Devices, 1994, 41(2):

233

- [4] Bousnina S, Mandeville P, Kouki A B, et al. A new analytical and broadband method for determining the HBT small-signal model parameters. *IEEE MTT-S Digest*, 2000: 1397
- [5] Ouslimani A, Gaubert J, Hafdallah H, et al. Direct extraction of linear HBT-model parameters using nine analytical expression blocks. *IEEE Trans Microw Theory Tech*, 2002, 50(1): 218
- [6] Bousnina S, Mandeville P, Kouki A B, et al. Direct parameter-extraction method for HBT small-signal model. *IEEE Trans Microw Theory Tech*, 2002, 50(2): 529
- [7] Lee K, Choi K, Kook S H, et al. Direct parameter extraction of SiGe HBTs for the VBIC bipolar compact model. *IEEE Trans Electron Devices*, 2005, 52(3): 375
- [8] Gao J, Li X, Wang H, et al. Approach for determination of extrinsic resistance for equivalent circuit model of metamorphic InP/InGaAs HBTs. *IEE Proc Microw Antennas Propag*, 2005, 152(3): 195
- [9] Dousset D, Issaoun A, Ghannouchi F M, et al. Wideband closed-form expressions for direct extraction of HBT small-signal parameters for all amplifier bias classes. *IEE Proc Circuits Devices Syst*, 2005, 152(5): 441
- [10] Gao J, Li X, Wang H, et al. An approach to determine small-signal model parameters for InP-based heterojunction bipolar transistors. *IEEE Trans Semicond Manuf*, 2006, 19(1): 138
- [11] Degachi L, Ghannouchi F M. Systematic and rigorous extraction method of HBT small-signal model parameters. *IEEE Trans Microw Theory Tech*, 2006, 54(2): 682
- [12] Yang T R, Tsai J M L, Ho C L, et al. SiGe HBT's small-signal Pi modeling. *IEEE Trans Microw Theory Tech*, 2007, 55(7): 1417
- [13] Gummel-Poon bipolar model description parameter extraction. [http://eesof.tm.agilent.com/docs/iccap2002/MDLGBOOK/7D\\_EVICE\\_MODELING/3TRANSISTORS/1GummelPoon/GP\\_DOCU.pdf](http://eesof.tm.agilent.com/docs/iccap2002/MDLGBOOK/7D_EVICE_MODELING/3TRANSISTORS/1GummelPoon/GP_DOCU.pdf)
- [14] Laser A P, Pulfrey D L. Reconciliation of methods for estimating  $f_{\max}$  for microwave heterojunction transistors. *IEEE Trans Electron Devices*, 1991, 38(8): 1685
- [15] Taurus-device TM user guide. Version W-2004.09, September 2004